DOI: 10.1002/chem.200600487

Self-Assembly and Liquid-Crystalline Properties of 5-Fluoroalkylporphyrins

Li-Mei Jin,[a] Juan-Juan Yin,[a] Liang Chen,[b] Jin-Ming Zhou,[a] Ji-Chang Xiao,[a] Can-Cheng Guo,*[b] and Qing-Yun Chen*[a, b]

Abstract: We report three crystal structures of a synthetic 5-fluoroalkylporphyrin molecule that was programmed for self-assembly. All the X-ray structures of zincated and free-base porphyrins **Zn2b**, **Zn5a**, and **2b** revealed rigorous π–π stacking and extremely hydrophobic interactions. Other the other hand, the strong aggregation of 5-fluoroalkylporphyrins in solution was also found. Interestingly, the regular nanopore formation of the 5-fluoroalkylporphyrin was visualized by atomic force microscopy (AFM). Importantly, the 5-fluoroalkylporphyrins possess liquid-crystalline properties that were confirmed by using a combination of differential scanning calorimetry (DSC) and polarizing optical microscopy (POM) techniques. By comparison, the self-assembly of non-fluorine-containing porphyrins with similar structure showed much lower aggregation ability, as investigated by NMR techniques. Additionally, no birefringent mesophase was observed for the non-fluorine-containing porphyrin.

Keywords: fluoroalkylporphyrins · liquid crystals · porphyrinoids · self-assembly · X-ray diffraction

Introduction

Supramolecular multiporphyrin assemblies with unique structural and functional properties provide attractive model systems in the study of various biological and chemical processes and in the design of new materials and devices.[1] Owing both to their planarity and high polarizability, porphyrins often show a strong tendency to self-aggregate and to form highly complex nanostructures.[2] Per(poly)fluorocarbons and per(poly)fluoroalkylated materials have attracted interest due to their technological relevance, and to special physical and chemical properties.[3] They also show a strong propensity to self-assemble into a variety of stable colloidal and supramolecular systems because of their extreme hydrophobicity (as well as lipophobicity).[4] Fluoroalkylporphyrins, composed of both fluoroalkyl and porphyrin units, have demonstrated many applications in catalytic and medical areas.[5] However, the self-assembly of fluoroalkylporphyrins, which might have the most promising self-association properties, has not yet been reported. Since our recent report of a series of new methods to synthesize various fluoroalkylporphyrins, we have been able to study their assembly and applications.[6] Herein, we describe our preliminary results of the supramolecular assembly of easily available fluoroalkylporphyrins in solution. Furthermore, the X-ray analysis revealed self-assembly of the fluoroalkylporphyrins in the solid state, and atomic force microscopy (AFM) revealed the formation of regular two-dimensional arrays on the substrate. The fluoroalkylporphyrins are a new class of liquid-crystal materials, as confirmed by a combination of differential scanning calorimetry (DSC) and polarizing optical microscopy (POM) techniques.

[a] Dr. L.-M. Jin, J.-J. Yin, J.-M. Zhou, J.-C. Xiao, Prof. Q.-Y. Chen
Key laboratory of Organofluorine Chemistry
Shanghai Institute of Organic Chemistry
Chinese Academy of Sciences
354 Fenglin Road, 200032, Shanghai (China)
Fax: (+86) 21-6416-6128
E-mail: Chenqy@mail.sioc.ac.cn

[b] Dr. L. Chen, Prof. C.-C. Guo, Prof. Q.-Y. Chen
College of Chemistry and Chemical Engineering
Hunan University
410082, Changsha (China)
Fax: (+86) 731-8821603
E-mail: ccguo@hnu.net.cn

Results and Discussion

Synthesis: All the porphyrins used in the self-assembly are shown in Scheme 1.

As illustrated in Scheme 2, zincated 5-fluoroalkylated porphyrins (**Zn2a–c**)[6b] can be easily synthesized from 5,15-diphenylporphinatozinc(II) (**Zn1**)[7] and fluoroalkyl iodides (R_FI). For example, the treatment of **Zn1** with 1.1 equivalents of R_FI in the presence of 1.1 equivalents of $Na_2S_2O_4$ in

Pagination corrected Oct. 17, 2006

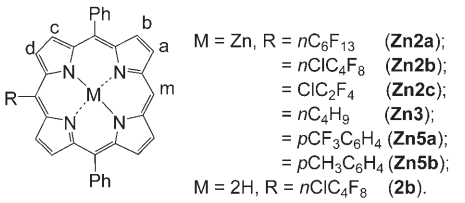

Scheme 1.

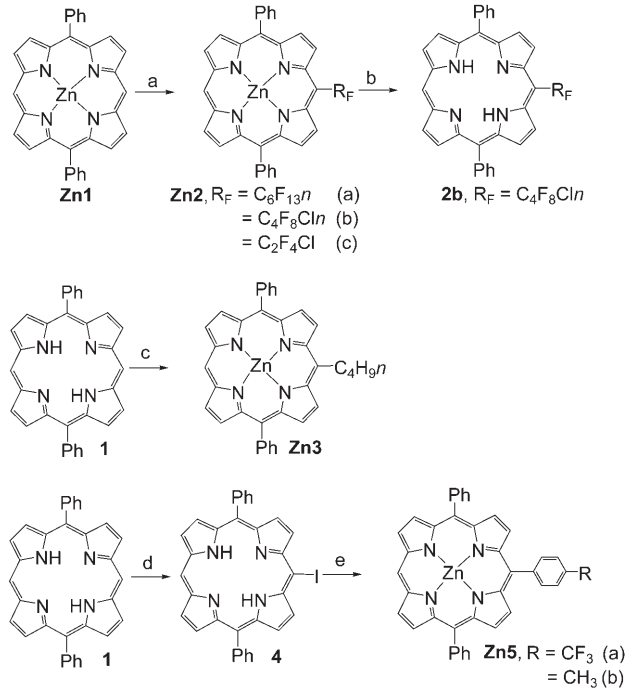

Scheme 2. Synthesis of 5-substituted porphyrins used in the self-assembly. a) Yield: 30–40%; i) R_FI, $Na_2S_2O_4$, DMSO/TFH/H_2O, 1 h, RT, then aqueous HCl (37%), 10 min, chromatography; ii) $Zn(OAc)_2$, CH_2Cl_2/MeOH, RT, 1 h, chromatography. b) Yield: quantitative; aqueous HCl (37%), CH_2Cl_2, 10 min. c) Yield: 50%; i) *n*BuLi, −78°C, THF, 10 min, then dichlorodicyanobenzoquinone (DDQ), RT, 30 min; ii) $Zn(OAc)_2$, RT, CH_2Cl_2, 30 min. d) Yield: 60%; I_2, phenyliodide bistrifluoroacetate (PIFA), CH_2Cl_2, 1 h. e) Yield: 90%; i) $ArB(OH)_2$, $[Pd(PPh_3)_4]$, K_2CO_3, toluene, 100°C, 4 h; ii) $Zn(OAc)_2$, CH_2Cl_2/MeOH, RT, 1 h.

a solvent mixture of THF/DMSO/H_2O (10:10:1, v/v) at 35°C for about 1 h, followed by demetalation with concentrated HCl (for easy separation of monofluoroalkylated product from starting porphyrin and minor bis(fluoroalkyl)-porphyrins) yielded free-base **2**, although this was contaminated with minor β-fluoroalkylated porphyrin. However, after they were metalated again with $Zn(OAc)_2$, followed by purification using dry powder column chromatography (300–400 mesh, SiO_2), the pure **Zn2** was obtained. Furthermore, the zincated product can be converted into corresponding free-base **2** quantitatively with concentrated HCl. 5-Butyl-10,20-diphenylporphyrin **3** was obtained by the reaction of free-base 5,15-diphenylporphyrin **1**[7] and *n*BuLi according to Senge's procedure.[8] After metalation with $Zn(OAc)_2$, 5-butyl-10,20-diphenylporphinatozinc(II) **Zn3** was obtained quantitatively. The compound 5-(4-trifluoromethylphenyl)-10,20-diphenylporphyrin **5a** was prepared by the reaction of 5-iodoporphyrin **4**[9] with 4-(trifluoromethyl)phenylboronic acid in the presence of 10 mol% $[Pd(PPh_3)_4]$ and K_2CO_3 in toluene at 100°C for 2 h, in 90% yield under Suzuki reaction conditions.[6d] 5-Iodoporphyrin **4** was readily available from the reaction of free-base **1** and I_2 and phenyliodide bistrifluoroacetate (PIFA) by using Dolphin's method.[9] Similarly, 5-(4-methylphenyl)-10,20-diphenylporphyrin **5b** was also synthesized by the reaction of **4** and *p*-tolylboronic acid, in 90% yield. The corresponding zincated complexes **Zn5a** and **Zn5b** were easily obtained by treating **5a** and **5b**, respectively, with $Zn(OAc)_2$.

Self-assembly behavior of 5-fluoroalkylporphyrins: Due to their excellent solubility,[10], the self-aggregation behavior of the zincated fluoroalkylporphyrins **Zn2a–c** and **Zn5a** was investigated quantitatively by monitoring the concentration dependence of the ^{1}H NMR chemical shifts in $CDCl_3$. For example, as the concentration changed from 130 to 4 mM, the chemical shifts of the m-, a-, b-position protons of **Zn2a** shift to downfield by 1.52, 0.9, and 0.66 ppm, respectively, suggesting stacking in the solution (Figure 1). Additionally, these results were compared to those of non-fluorine-containing porphyrins **Zn3** and **Zn5b**. Table 1 lists the chemical-shift changes of the corresponding protons of all the por-

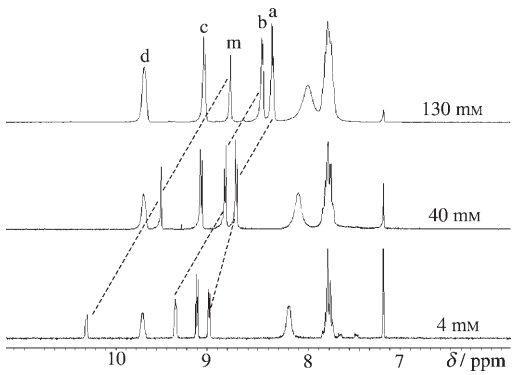

Figure 1. Aromatic region of the 300 MHz ^{1}H NMR spectrum of **Zn2a** in $CDCl_3$; the residual $CHCl_3$ peak is at $\delta = 7.26$ ppm; the assignment of the protons is based on NOESY spectra.

Table 1. ^{1}H NMR chemical-shift changes (300 MHz, ppm) of all the porphyrins in $CDCl_3$ at 25°C as the concentration changed from 130 to 4 mM.

Entry	Compound	Δδ m-H[a]	Δδ a-H	Δδ b-H	Δδ c-H	Δδ d-H
1	**Zn2a**	1.52	0.9	0.66	<0.01	<0.01
2	**Zn2b**	1.37	0.85	0.58	0.06	<0.01
3	**Zn2c**[b]	0.34	0.23	0.12	<0.01	<0.01
4	**Zn3**	0.53	0.36	0.16	0.13	0.3
5	**Zn5a**	0.8	0.5	0.3	<0.01	<0.01
6	**Zn5b**	~0.1	~0.07	<0.01	<0.01	<0.01
7	**2b**[c]	0.12	0.08	<0.01	<0.01	<0.01

[a] $\Delta\delta = \delta_{4mM} - \delta_{130mM}$, the upfield shifts due to shielding effect. [b] The concentration changed from 16 to 1.6 mM due to its low solubility. [c] The concentration changed from 75 to 7 mM.

phyrins. Compounds **Zn2a–c** and **Zn5a** revealed strong concentration dependence in the ^{1}H NMR spectra, occurring at much higher values than in the cases of **Zn3** and **Zn5b**, which indicates more aggregation in **Zn2a–c** and **Zn5a**.

The fact that only the pyrrolic protons remote from the fluoroalkyl or trifluoromethylphenyl group in **Zn2a–c** and **Zn5a** showed strong self-association in $CDCl_3$ indicates that the coordination of the zinc atom by the fluorine atom can be ruled out. In fact, the presence of the zinc atom is not mandatory for this stacking. The shifts toward higher field as the concentration increased were also observed for the same protons in the free-base **2b**, although the effects are much weaker (Table 1, entry 7). We thought that the strong self-association ability of fluoroalkylporphyrin is mainly attributed to the extremely strong hydrophobic interactions of the fluoroalkyl tails between the neighboring fluoroalkylporphyrins.

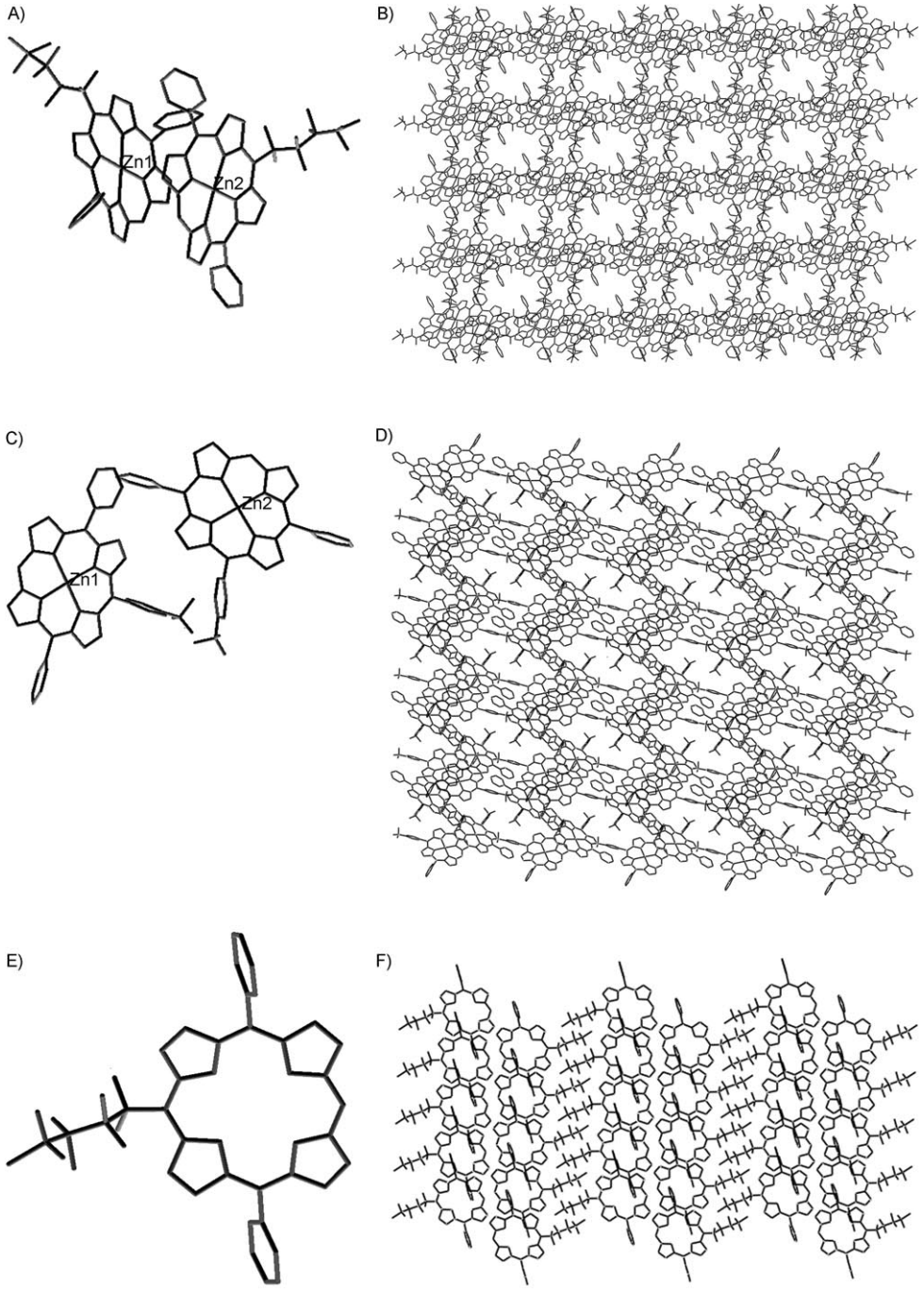

Figure 2. A) Crystal structure of (**Zn2b**)$_2$; B) crystal-packing diagram of **Zn2b** ($a=5$, $b=1$, $c=5$); C) crystal structure of (**Zn5a**)$_2$; D) crystal-packing diagram of **Zn5a** ($a=5$, $b=1$, $c=5$); E) crystal structure of **2b**; F) crystal-packing diagram of **2b** ($a=5$, $b=1$, $c=3$). Hydrogen atoms and disordered positions have been omitted for clarity.

Table 2. Crystal data and experimental parameters of the structural analysis.

Compound	**Zn2b**	**Zn5a**	**2b**
formula weight	1520.74	1399.96	697.02
crystal system	triclinic	triclinic	triclinic
space group	$P\bar{1}$	$P\bar{1}$	$P\bar{1}$
T [K]	293 (2)	293 (2)	293 (2)
a [Å]	13.8062(14)	14.0836(14)	6.6339(10)
b [Å]	14.6219(15)	14.1606(15)	10.4240(15)
c [Å]	17.8229(18)	17.6627(18)	22.688(3)
α [°]	113.056(2)	110.813(2)	96.857(3)
β [°]	92.479(2)	92.324(2)	92.791(3)
γ [°]	107.107(2)	107.591(2)	100.305(3)
V [Å^3]	3112.3(5)	3095.1(5)	1528.6(4)
Z	4	4	2
μ ($Mo_{K\alpha}$) [mm^{-1}]	0.958	0.847	0.209
ρ_{calcd} [g cm^{-3}]	1.623	1.438	1.514
no. collected reflns	16591	18445	8110
no. unique reflns	11429	13126	5597
R_{int}	0.0936	0.097	0.1442
no. reflns with $I>2\sigma$	11429	13126	5597
no. refined parameters	901	848	485
GOF [$I>2\sigma(I)$]	0.883	0.743	1.036
R [$I>2\sigma$]	0.0913	0.0646	0.1071
R [all data]	0.1863	0.2351	0.1414
Rw [$I>2\sigma$]	0.2356	0.1253	0.2736
Rw [all data]	0.2866	0.2067	0.3049
$\lvert\Delta\rho\rvert_{max}$ [e Å^{-3}]	0.873	0.585	0.46

To gain deeper insight into the role of the fluoroalkyl group in the self-association, the single-crystal structures of **Zn2b**, **Zn5a**, and **2b** were determined by X-ray diffraction. **Zn2b**, **Zn5a**, and **2b** all yielded triclinic crystals from CH_2Cl_2/hexane. Interestingly, the X-ray structures of **Zn2b** and **Zn5a** revealed rigorous stacking and π-complexation in the solid state. As expected, the fluoroalkyl group in **Zn2b** and **Zn5a** has a dramatic effect upon the stability of the resulting π-complexation of these compounds in the solid state. As seen from the crystal structures (Figure 2A, C, E and Table 2), the minimal unit of **Zn2b** or **Zn5a** has two independent porphyrin units that account for the dimeric molecular ion peak determined by mass spectroscopy (MALDI). Offset face-to-face π-stacking interactions are observed in the crystal cell diagram, and these link the minimal unit (dimer) into tetramers with an interplane separation of 3.34 Å and centroid···centroid distance of 4.47 Å between the close parallel porphyrin plane for **Zn2b** (the shortest F···F distance between two neighboring fluoroalkyl tails is 2.75 Å, shorter than the sum of the corresponding van der Waals radii 2.9 Å)[11] and an interplane separation of 3.37 Å and centroid···centroid distance of 4.44 Å for **Zn5a**. Interestingly, as seen from the *b* axis, a regular two-dimensional-network array is formed for **Zn2b** and **Zn5a** (Figure 2B, D, respectively). Furthermore, two-dimensional-network arrays of other functional porphyrins in the solid state have been previously achieved through the interplanar hydrogen bond.[12] The fluoroalkyl group in **2b** also plays a important role in the self-assembly. In contrast to that of **Zn2b** and **Zn5a**, the endless one-dimensional chains of **2b** were formed through the *c* axis by the hydrophobic interactions of fluoroalkyls (the shortest distance of F···F between two neighboring fluoroalkyl tailors is 2.87 Å, slightly shorter than the sum of the corresponding van der Waals radii) and π-stacking of the porphyrin plane with interplane separation of 3.37 Å and a centroid···centroid distance of 10.505 Å (Figure 2F). The relatively large distance between the two neighboring porphyrins might explain the weak self-assembling effect found in solution.

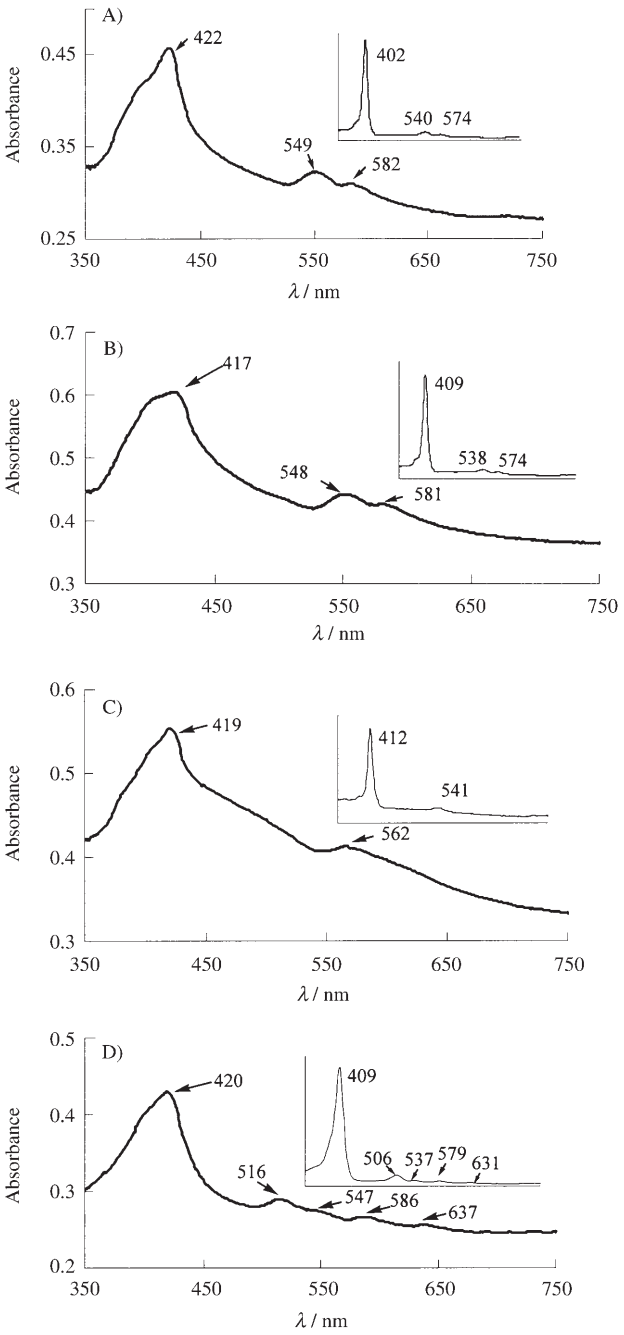

Figure 3. UV/Vis spectra of the self-assembled porphyrins. A) **Zn2a** in the crystal state; inset: **Zn2a** in CH_2Cl_2; B) **Zn2b** in the crystal state; inset: **Zn2b** in CH_2Cl_2; C) **Zn5a** in the crystal state; inset: **Zn5a** in CH_2Cl_2; D) **2b** in the crystal state; inset: **2b** in CH_2Cl_2.

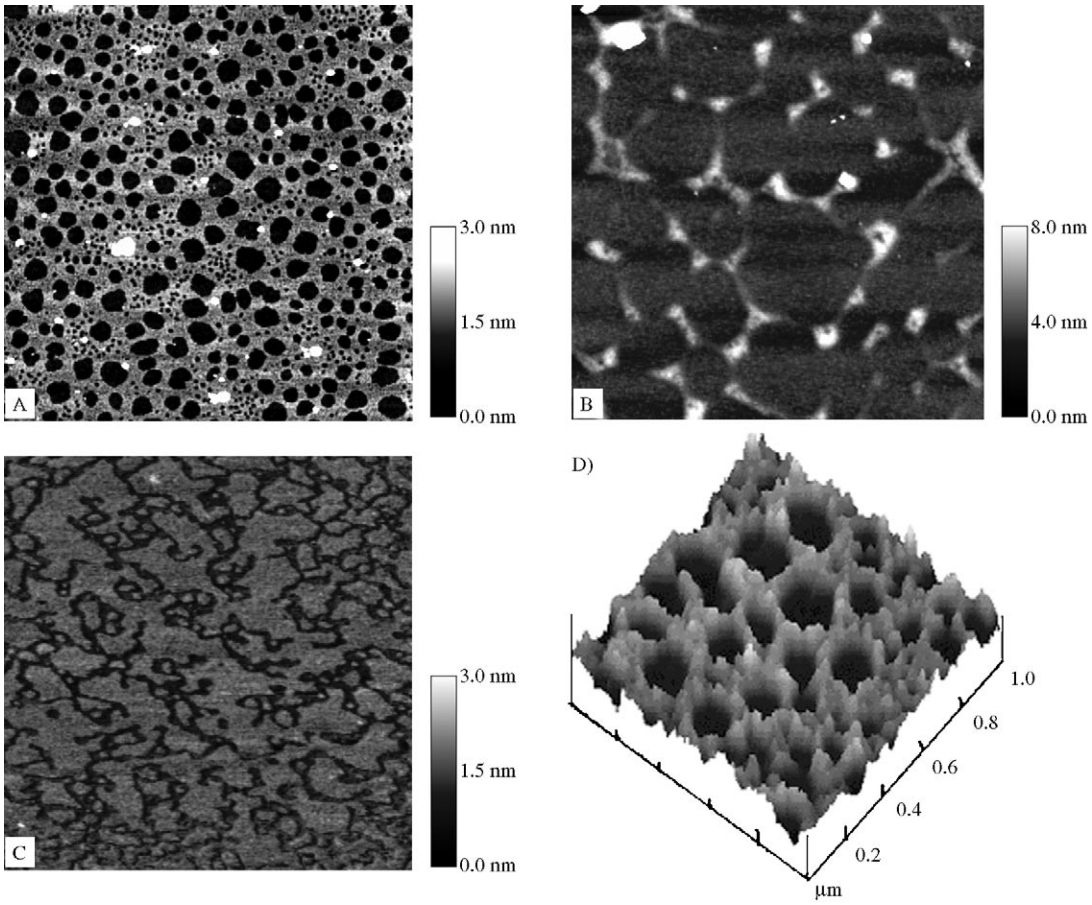

Figure 4. Tapping-mode AFM overview images of A) **Zn2a**: scan area: 5×5 µm, scale bar: 3 nm. The average height is 1.48 nm. The sample was prepared on a clean mica by putting one drop of a solution of **Zn1a** in dry chloroform on the chip and allowing the solvent to evaporate in air; B) **Zn5a**: scan area: 5×5 µm, scale bar: 8 nm. Sample preparation as above; C) **Zn3**: scan area: 1×1 µm, scale bar: 3 nm. Sample preparation as above. Tapping-mode AFM height images of sample on mica substrate from a 0.7 mM solution. Note: amorphism rather than nanopore formation of the self-assemblies. D) Detail from the image in (A) shown in 3D mode, but in topographic representation, scan area: 1×1 µm.

Attempts to obtain suitable crystals of compound **Zn2a** for diffraction analysis failed, however the absorption spectra of the resulting small crystals in the solid state could be determined.[10a,13] As shown in Figure 3A, the self-assembly of **Zn2a** in the solid state produces characteristic effects. Indeed, a UV-visible spectrum of microcrystals between two quartz plates shows strong excitonic interactions, with a broadening of the Soret band, together with bathochromic shifts in the Q bands. The absorption maxima for a Soret band and two Q-bands appear at 422, 549, and 582 nm, respectively, and the corresponding bands obtained in the homogeneous CH_2Cl_2 solution appear at 409, 540, and 574 nm. The shapes of the absorption spectra for other crystals of **Zn2b**, **Zn5a**, and **2b** (Figure 3B–D, respectively) were similar to that for **Zn2a**.

After having gained information about the self-association of fluoroalkylporphyrins in solution and in crystals, we investigated the self-association morphology of **Zn2a** and **Zn5a** on the substrate by using the AFM technique. Thus, the samples were first prepared by depositing them on the mica from their $CHCl_3$ solution at room temperature. Interestingly, the regular nanopores for them were obtained (Figure 4A, B, D). On the other hand, **Zn3** film from solution of the same concentration was completely amorphous (Figure 4C).

Thermal behavior of fluoroalkylporphyrins: The strong self-association ability of the fluoroalkylporphyrins prompted us to check their mesomorphic behavior. The thermal behavior of **Zn2a**, **Zn2b**, **2b**, and **Zn3** was characterized by DSC and POM. The DSC thermograms showed that all samples, except **Zn2a**, are thermally stable. Importantly, all the fluoroalkylporphyrins (**Zn2a**, **Zn2b**, **2b**) exhibit an enantiotropic mesophase, however, decomposition of **Zn2a** occurred at around its melting point (~220 °C). The melting transition temperature of 135 °C for **Zn2a** was observed during its first heating scan, however, in the second heating scan, the porphyrin resulting from **Zn2a** could not be melted, even at temperatures greater than 350 °C. The melting transition temperature of 149 °C for **2b** is lower than that of 166 °C for **Zn2b** collected from the second heating scan (Figure 5).

Mesophase textures were identified by microscopy observations. After fast cooling of the isotropic-state samples

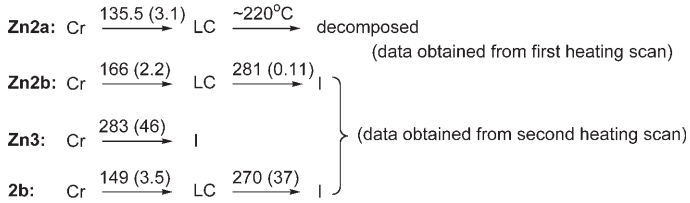

Figure 5. Phase behaviors of **Zn2a**, **Zn2b**, **Zn3**, and **2b**. The transition temperature (°C) and enthalpies (in parentheses, $J\,g^{-1}$) were determined by DSC at a rate of $10\,°C\,min^{-1}$. Cr, crystalline phase; LC, liquid-crystal phase; I, isotropic.

from 300 to 50 °C at the rate of $120\,°C\,min^{-1}$, then slow heating of the annealed sample to 300 °C at the rate of $10\,°C\,min^{-1}$, textures generally associated with columnar mesophase were observed, starting at about 150 °C for **2b** and about 210 °C for **Zn2b** under POM (Figure 6A, B). These textures did not transfer into the corresponding isotropic state until they were heated to their melting point. Again, consistent with the result from DSC measurement, no birefringent mesophase was observed for **Zn3** (not shown in Figure 6).

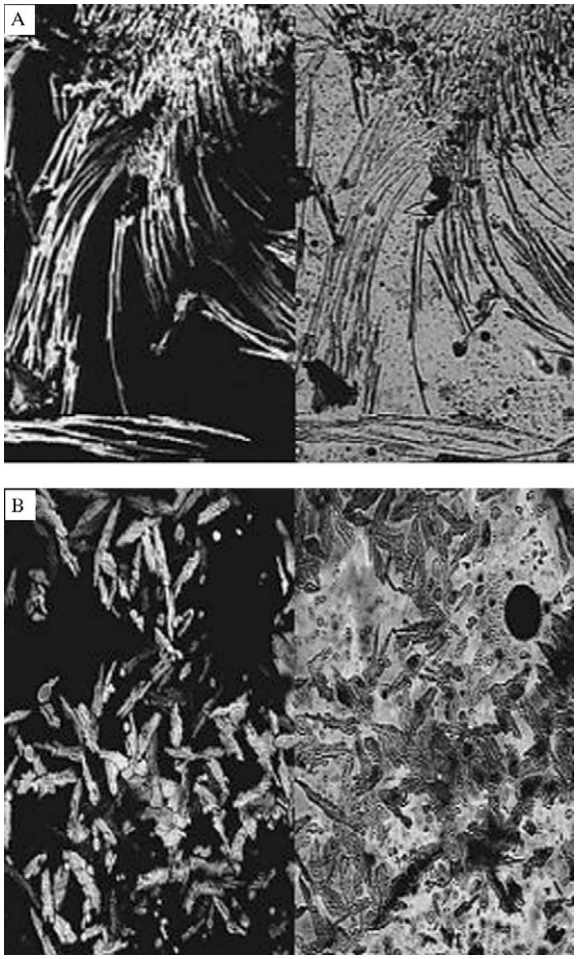

Figure 6. A) Optical texture (magnification × 100) of **2b** (left with and right without cross-polarizer). B) Optical texture (magnification × 100) of **Zn2b** (left with and right without cross-polarizer).

Conclusion

The excellent self-assembly and thermal behavior characteristics of fluoroalkylporphyrins have been demonstrated for the first time. The strong aggregation of fluoroalkylporphyrins was found not only in solution, but also in crystals. Furthermore, the AFM determination showed nanopore formation on the mica for these fluoroalkylporphyrins. Importantly, the fluoroalkylporphyrins are a new class of liquid-crystal materials, as verified by a combination of differential scanning calorimetry (DSC) and polarizing optical microscopy (POM) techniques. This research may open a new vista in materials and devices using fluoroalkylporphyrins.

Experimental Section

General: ^{1}H NMR spectra were measured by using a Bruker 300 spectrometer operating at 300 MHz with TMS internal standard as a reference for chemical shifts. Thermal behavior was determined by using a PYRIS 1 DSC system at a scanning rate of $5\,°C\,min^{-1}$ under nitrogen. Liquid-crystalline textures were observed under a LEICA-DMLP polarized optical microscope (POM). The compounds of **Zn2a–c**,[6b] **2b**,[6b] **Zn3**,[8] **Zn5a**,[6d] and **Zn5b**[6d] were synthesized according to previous methods.

X-ray diffraction studies: Crystallization of the compounds in small glass tubes was induced by slow evaporation of a solution of CH_2Cl_2 (4 mL) including ~10 mg porphyrins, covered with 2 mL hexane to yield translucent purple needles (after about 2 weeks). The X-ray measurements (Bruker AXS D8 diffractometer equipped with a SMART APEX CCD detector) were carried out at 293 K, on crystals coated with a thin layer of amorphous hydrocarbon oil to minimize deterioration, possible structural disorder, and related thermal-motion effects, and to optimize the precision of the crystallographic results. The crystal and experimental data for **Zn2b**, **Zn5a**, and **2b** are summarized in Table 2. These structures were solved and refined by full-matrix least-squares against F^2 (SHELXL-97).[14] All non-hydrogen atoms were refined anisotropically. In both **Zn2b** and **2b**, some of fluorine atoms at the end of the fluoroalkyl group chain were disordered. CCDC 603431 (for **Zn2b**), 603433 (for **Zn5a**), and 603432 (for **2b**) contain the supplementary crystallographic data for this paper. These data can be obtained free of charge from The Cambridge Crystallographic Data Centre via www.ccdc.cam.ac.uk/data_request/cif.

AFM measurements: A drop of the porphyrin dissolved in dry chloroform was put on the clean mica and dried in air. All AFM investigations were performed by using a Multimode AFM system combined with a Nanoscope IIIa controller (Digital Instruments, USA), which was operated in tapping mode, using a fluid cell, J scanner and 200-μm cantilevers with Si_3N_4 tips.

Acknowledgements

We thank the National Nature Science Foundation of China for financial support (Nos. 20272026, 200302010, 20532040).

[1] a) T. S. Balaban, *Acc. Chem. Res.* **2005**, *38*, 612–623; b) J.-C. Chambron, V. Heitz, J.-P. Sauvage, *The Porphyrin Handbook* (Eds.: K. M. Kadish, K. M. Smith, R. Guilard), Academic Press, **2000**, Vol. 6, pp. 1–42; c) J.-H. Chou, H. S. Nalwa, M. E. Kosal, N. A. Rakow, K. S. Suslick, *The Porphyrin Handbook* (Eds.: K. M. Kadish, K. M. Smith, R. Guilard), Academic Press, **2000**, Vol. 6, pp. 43–132.

[2] a) T. S. Balaban, A. D. Bhise, M. Fischer, M. Linke-Schaetzel, C. Roussel, N. Vanthuyne, *Angew. Chem.* **2003**, *115*, 2190–2194; *Angew. Chem. Int. Ed.* **2003**, *42*, 2140–2144; b) T. S. Balaban, M. Linke-Schaetzel, A. D. Bhise, N. Vanthuyne, C. Roussel, C. E. Anson, G. Buth, A. Eichhöfer, K. Foster, G. Garab, H. Gliemann, R. Goddard, T. Javorfi, A. K. Powell, H. Rösner, T. Schimmel, *Chem. Eur. J.* **2005**, *11*, 2267–2275; c) R. Rotomskis, R. Augulis, V. Snitka, R. Valiokas, B. Liedberg, *J. Phys. Chem. B* **2004**, *108*, 2833–2838; d) T. Hasobe, S. Fukuzumi, P. V. Kamat, *J. Am. Chem. Soc.* **2005**, *127*, 11884–11885; e) P. Kubát, K. Lang, P. Janda, P. Anzenbacher, Jr., *Langmuir* **2005**, *21*, 9714–9720; f) S. George, I. Goldberg, *Cryst. Growth Des.* **2006**, *6*, 755–762.

[3] a) I. T. Horvath, J. Rabai, *Science* **1994**, *266*, 72–75; b) A. Studer, S. Hadida, R. Ferrito, S. Y. Kim, P. Jeger, P. Wipf, D. P. Curran, *Science* **1997**, *275*, 823–826; c) R. P. Hughes, S. M. Maddock, I. A. Guzei, L. M. Liable-Sands, A. L. Rheingold, *J. Am. Chem. Soc.* **2001**, *123*, 3279–3288.

[4] a) J. G. Riess, *Colloids Surf. A* **1994**, *84*, 33–48; b) M. P. Krafft, Riess, J. G. *Biochimie* **1998**, *80*, 489–514.

[5] a) S. G. DiMagno, P. H. Dussault, J. A. Schultz, *J. Am. Chem. Soc.* **1996**, *118*, 5312–5313; b) S. Mettath, G. Li, T. Srikrishnan, R. Mehta, Z. D. Grossman, T. J. Dougherty, R. K. Pandey, *Org. Lett.* **2001**, *1*, 1961–1964.

[6] a) L. M. Jin, Z. Zeng, C. C. Guo, Q. Y. Chen, *J. Org. Chem.* **2003**, *68*, 912–3917; b) L. M. Jin, L. Chen, J. J. Yin, C. C. Guo, Q. Y. Chen, *J. Fluorine Chem.* **2005**, *126*, 1321–1326; c) L. M. Jin, L. Chen, J. J. Yin, C. C. Guo, Q. Y. Chen, *J. Org. Chem.* **2006**, *71*, 527–536; d) L. M. Jin, J. J. Yin, L. Chen, C. C. Guo, Q. Y. Chen, *Eur. J. Org. Chem.* **2005**, 3994–4001.

[7] S. G. DiMagno, V. S. Y. Lin, M. J. Therien, *J. Org. Chem.* **1993**, *58*, 5983–5993.

[8] M. O. Senge, X. Feng, *J. Chem. Soc. Perkin Trans. 1* **2000**, *21*, 3615–3621.

[9] R. W. Boyle, C. K. Johnson, D. Dolphin, *J. Chem. Soc. Chem. Commun.* **1995**, 527–528.

[10] a) T. S. Balaban, A. Eichhöfer, J.-M. Lehn, *Eur. J. Org. Chem.* **2000**, 4047–4057; b) R. B. Martin, *Chem. Rev.* **1996**, *96*, 3043–3064; c) M. Kastler, W. Pisula, D. Wasserfallen, T. Pakula, K. Müllen, *J. Am. Chem. Soc.* **2005**, *127*, 4286–4296.

[11] A. Bondi, *J. Phys. Chem.* **1964**, *68*, 441–451.

[12] S. George, I. Goldberg, *Cryst. Growth Des.* **2006**, *6*, 755–762.

[13] S. Tanaka, M. Shirakawa, K. Kaneko, M. Takeuchi, S. Shinkai, *Langmuir* **2005**, *21*, 2163–2172.

[14] G. M. Sheldrick, SHELXL-97: Program for the Refinement of Crystal Structures from Diffraction Data, University of Göttingen, Germany, **1997**.

Received: April 6, 2006
Published online: July 28, 2006

